

Supporting Information

Facilitated gallium incorporation in blue-emitting $\text{In}_{1-x}\text{Ga}_x\text{P}$ alloy quantum dots via monomeric gallium precursors

Taewan Kim,^a Se-Yup Kim,^a Sooho Lee,^b Ji-Sang Park,^c Hyeyonjun Lee,^{*d} and Doh C. Lee^{*a}

^a Department of Chemical and Biomolecular Engineering, KAIST Institute for the Nanocentury, Energy and Environmental Research Center (EERC), KAIST Graduate School of Semiconductor Technology, Korea Advanced Institute of Science and Technology (KAIST), Daejeon 34141, Republic of Korea. E-mail: dclee@kaist.edu

^b Samsung Display Research Center, Samsung Display, Yongin, Republic of Korea

^c SKKU Advanced Institute of Nanotechnology (SAINT), Sungkyunkwan University (SKKU), Suwon 16419, Republic of Korea

^d Department of Energy Science and Center for Artificial Atoms, Sungkyunkwan University, Suwon 16419, Republic of Korea. E-mail: lhj9269@skku.edu

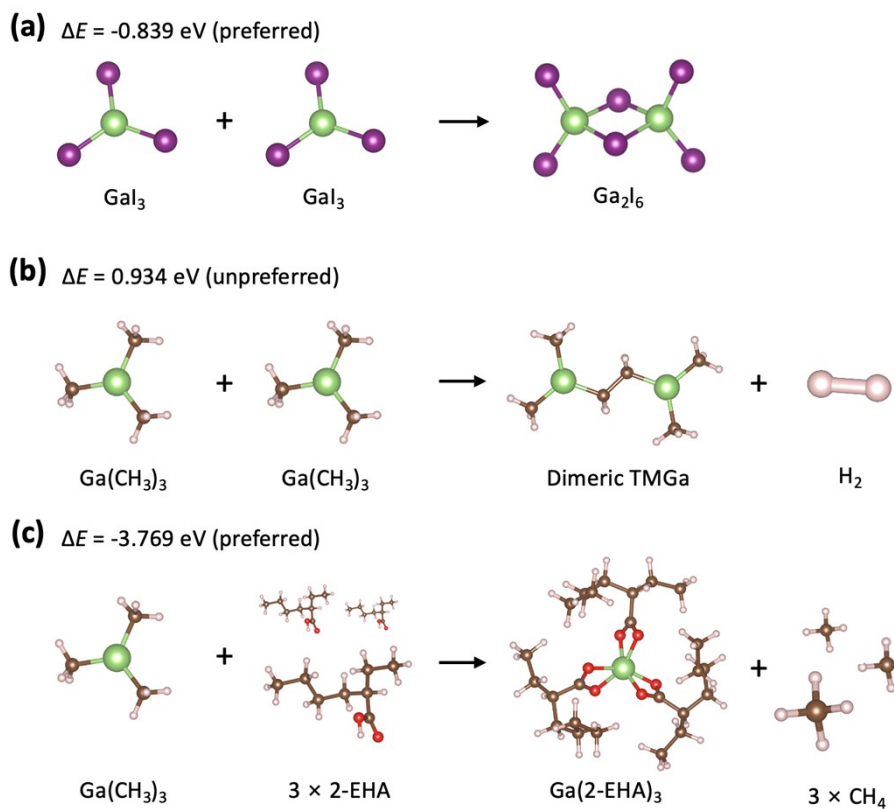


Fig. S1 Energy change (ΔE) for the reaction of the (a) dimerization of gallium iodide, (b) dimerization of TMGa, and (c) formation of gallium tri-2-ethylhexanoate from TMGa, calculated using first-principles density functional theory (DFT).

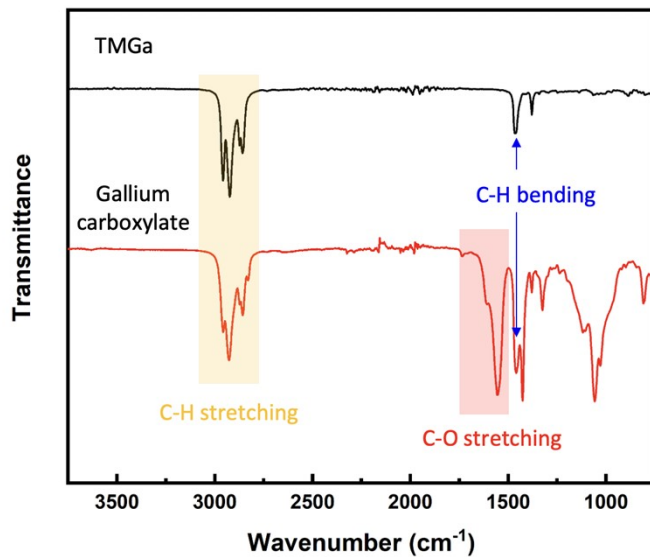


Fig. S2 FTIR spectra of gallium 2-ethylhexanoates derived from TMGa. Four equivalents of 2-EHA were reacted with TMGa.

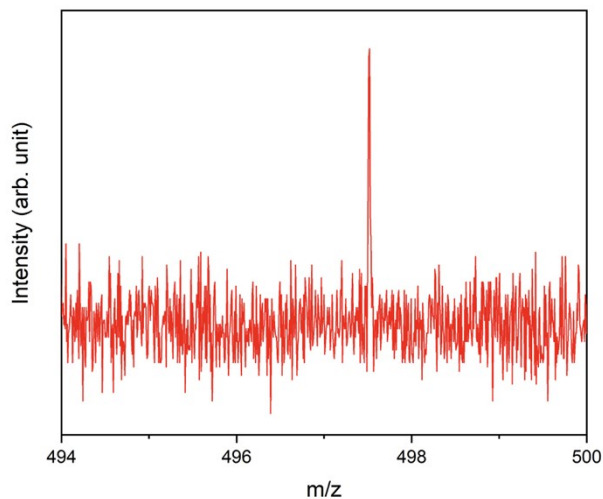


Fig. S3 LDI-TOF spectra of gallium 2-ethylhexanoates synthesized by the reaction of TMGa with 2-EHA.

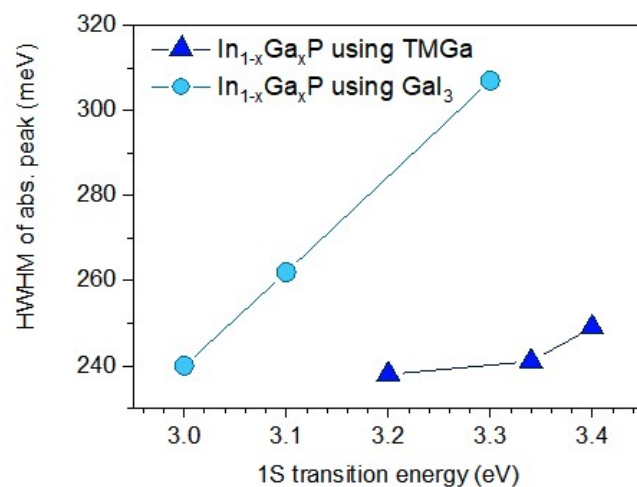


Fig. S4 HWHM values of the absorption peak of $\text{In}_{1-x}\text{Ga}_x\text{P}$ QDs according to their 1S transition peak energies. The HWHM values are shown for QDs derived from TMGa (sky blue) and gallium iodide (blue) at different Ga-to-In feed ratios.

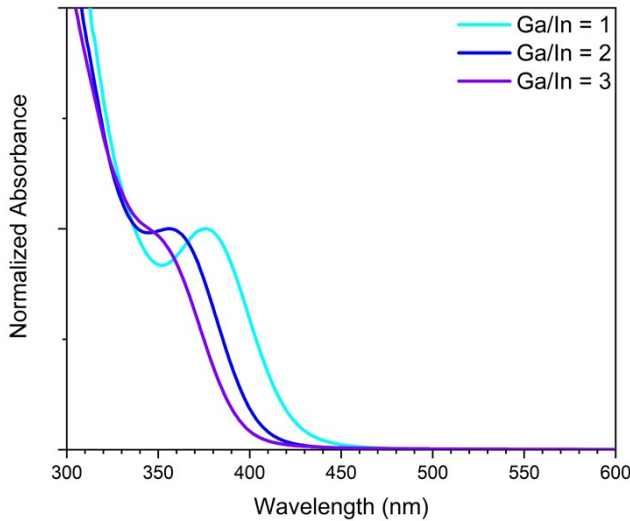


Fig. S5 UV-vis absorption spectra of $\text{In}_{1-x}\text{Ga}_x\text{P}$ cores synthesized from $\text{Ga}(\text{acac})_3$ with different Ga-to-In feed ratios.

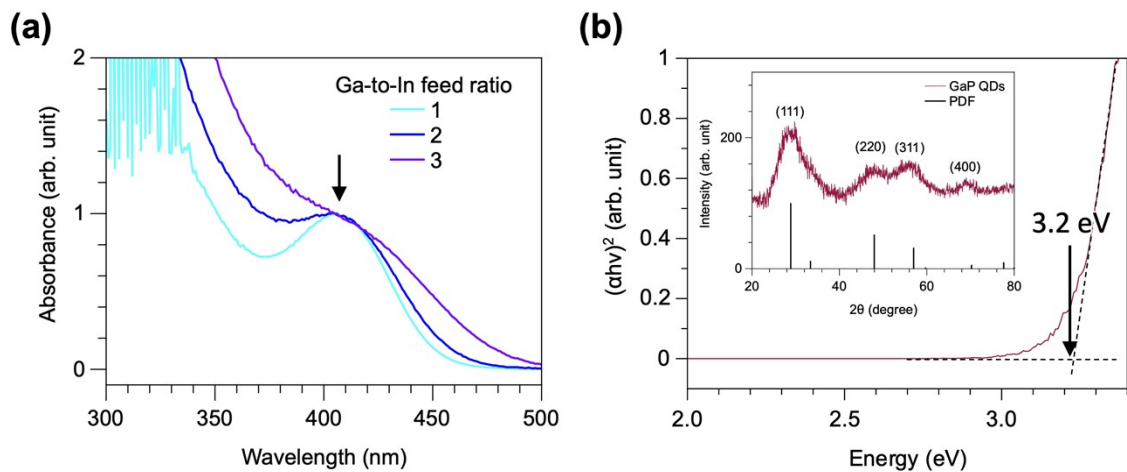


Fig. S6 Characterization of $\text{In}_{1-x}\text{Ga}_x\text{P}$ and GaP QDs using di-substituted gallium carboxylate derived from TMGa. (a) Absorption spectra of $\text{In}_{1-x}\text{Ga}_x\text{P}$ QDs using $\text{Ga}(\text{CH}_3)(\text{LA})_2$ with different Ga-to-In feed ratios. The black arrow indicates the 1S transition peak of the QDs (b) Tauc plot of GaP QDs using $\text{Ga}(\text{CH}_3)(\text{LA})_2$. The black arrow indicates the optical band gap of GaP QDs. The inset shows the XRD pattern for the GaP QDs (red) and standard peaks for GaP (JCPDS #32-0397, vertical lines).

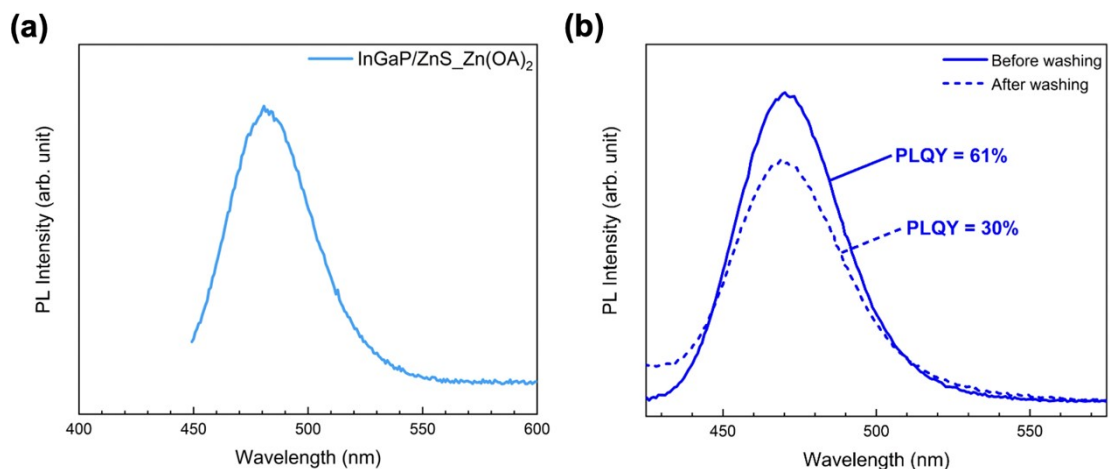


Fig. S7 PL properties of $\text{In}_{1-x}\text{Ga}_x\text{P}/\text{ZnS}$ QDs according to Zn precursors. (a) PL spectrum of $\text{In}_{1-x}\text{Ga}_x\text{P}/\text{ZnS}$ QDs synthesized using $\text{Zn}(\text{OA})_2$ as the only Zn precursor for ZnS shell growth. (b) Change in the PL spectra and PL QYs of $\text{In}_{1-x}\text{Ga}_x\text{P}/\text{ZnS}$ QDs synthesized by ZnCl_2 -OAm depending on the purification process.

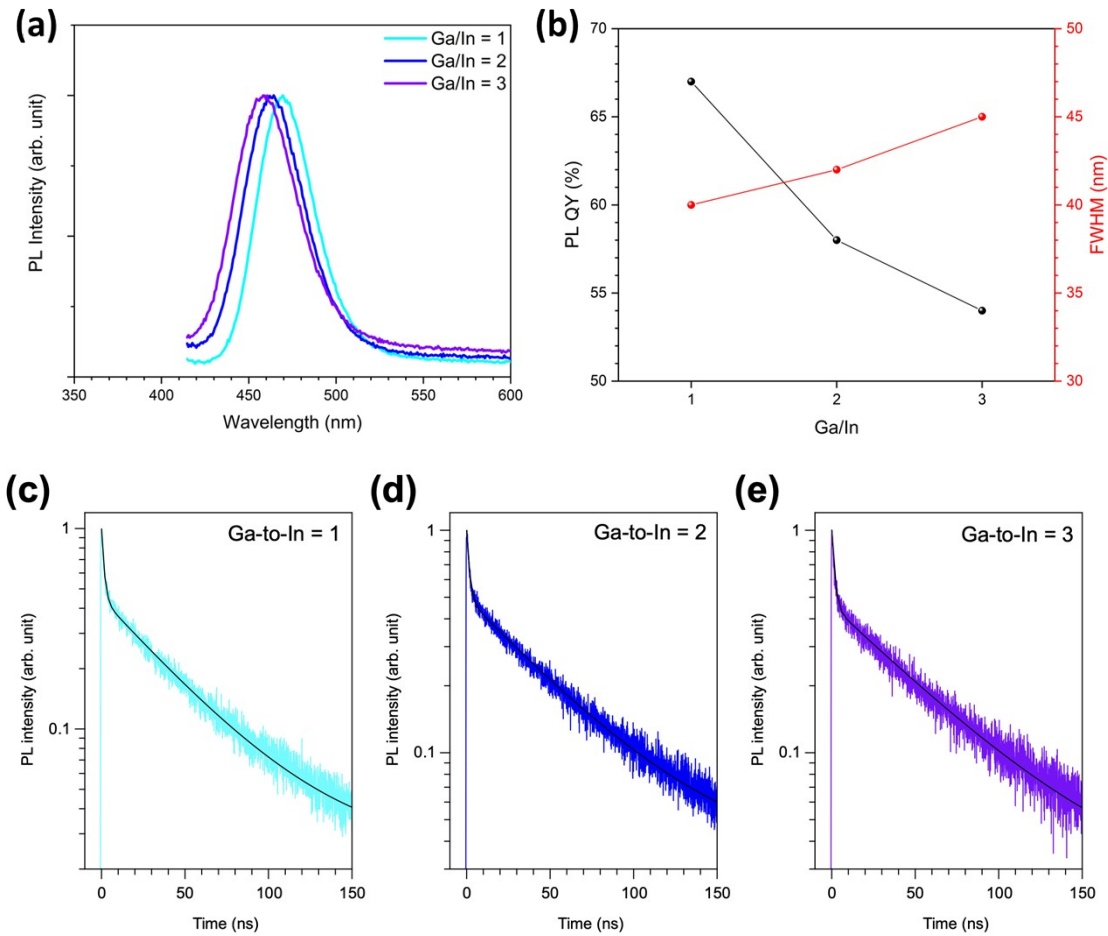


Fig. S8 PL properties of $\text{In}_{1-x}\text{Ga}_x\text{P}/\text{ZnS}$ QDs as function of Ga-to-In feed ratio. (a) Steady-state PL spectra of $\text{In}_{1-x}\text{Ga}_x\text{P}/\text{ZnS}$ QDs with varying Ga-to-In ratios (1, 2, and 3). (b) PL QY and FWHM of $\text{In}_{1-x}\text{Ga}_x\text{P}/\text{ZnS}$ QDs for Ga-to-In ratios of 1, 2, and 3. (c–e) Time-resolved PL decay curves of $\text{In}_{1-x}\text{Ga}_x\text{P}/\text{ZnS}$ QDs with Ga-to-In ratios of (c) 1, (d) 2, and (e) 3. Black solid lines represent the biexponential fits using the function $y = A_1 e^{-t/\tau_1} + A_2 e^{-t/\tau_2}$.

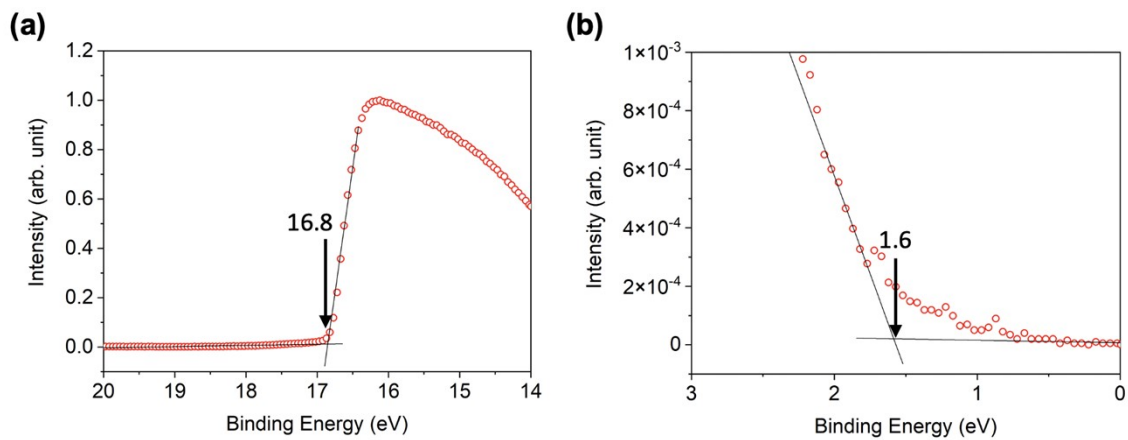


Fig. S9 UPS spectra for (a) secondary electron cutoff and (b) valence band edge regions of $\text{In}_{1-x}\text{Ga}_x\text{P}/\text{ZnS}$ QDs.

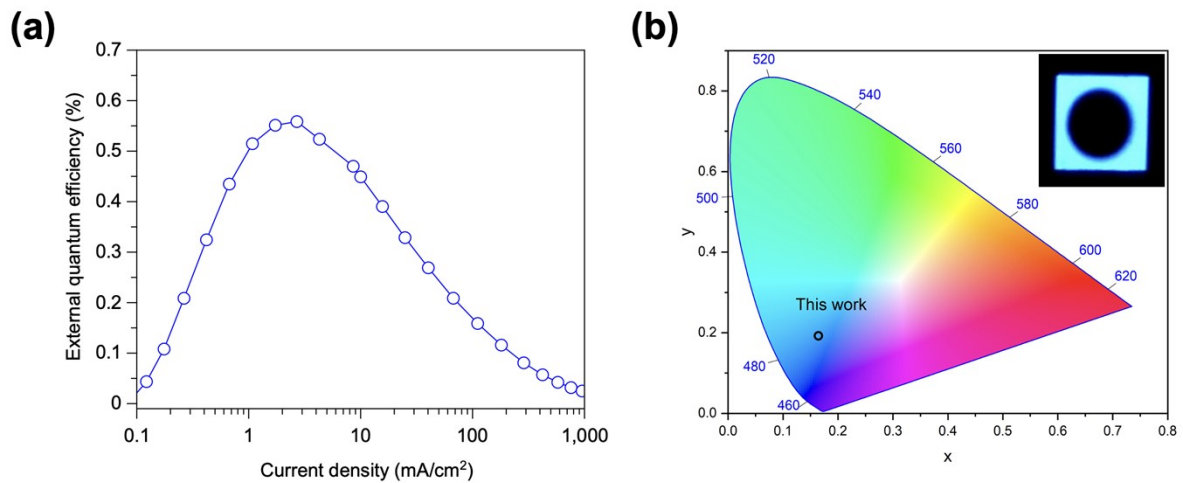


Fig. S10 (a) External quantum efficiency (EQE)–current density characteristics of $\text{In}_{1-x}\text{Ga}_x\text{P}/\text{ZnS}$ QD-based QLEDs. (b) Chromaticity diagram of $\text{In}_{1-x}\text{Ga}_x\text{P}/\text{ZnS}$ QD-based QLEDs on CIE 1931 coordinates. Inset shows a photograph of QLEDs in operation at 5 V.

Table S1 Summary of the elemental analysis for gallium 2-ethylhexanoate derived from gallium iodide (i.e., $\text{Ga}_2\text{I}_2(2\text{-EHA})_4$, synthesized with a gallium iodide-to-2-ethylhexanoic acid ratio of 1:4)

Elements	C	H	O
Expected mass percentage (%)	39.2	6.7	13.2
Measured mass percentage (%)	36.0	6.6	20.1

Table S2 Molar ratio (%) of Zn, In, Ga, and P in $\text{In}_{1-x}\text{Ga}_x\text{P}$ QDs characterized by ICP-OES results

	using $\text{Ga}(\text{LA})_3$				using $\text{Ga}(\text{CH}_3)(\text{LA})_2$			
	Zn	In	Ga	P	Zn	In	Ga	P
$\text{In}_{1-x}\text{Ga}_x\text{P}$ (2:1:1)	26.6	29.4	19.3	24.8	33.2	20.9	22.0	23.9
$\text{In}_{1-x}\text{Ga}_x\text{P}$ (2:0.67:1.33)	28.4	18.0	27.4	26.2	26.1	10.9	37.8	25.2
$\text{In}_{1-x}\text{Ga}_x\text{P}$ (2:0.5:1.5)	30.2	14.1	31.1	24.6	28.7	8.1	40.4	22.8

Table S3 PL decay fitting results of $\text{In}_{1-x}\text{Ga}_x\text{P}/\text{ZnS}$ QDs with different Ga-to-In feed ratios

Ga-to-In ratio	τ_1 (ns)	A ₁	τ_2 (ns)	A ₂
1	1.5	0.56	45.9	0.44
2	1.7	0.52	53.2	0.48
3	1.6	0.45	58.7	0.55

Table S4 Literature survey for the photoluminescence characteristics of $\text{In}_{1-x}\text{Ga}_x\text{P}$ QDs (emission at 430–500 nm)

Synthesis method	Structure	PL peak (nm)	PLQY (%)	FWHM (nm)	Reference
Cation exchange in organic solvents	$\text{In}_{1-x}\text{Ga}_x\text{P}/\text{ZnSeS}/\text{ZnS}$	465-475	80-82	47	1
	$\text{In}_{1-x}\text{Ga}_x\text{P}/\text{ZnSeS}/\text{ZnS}$	457	84	52	2
Cation exchange in molten salts	$\text{In}_{1-x}\text{Ga}_x\text{P}/\text{ZnS}$	497	30	50	3
	$\text{In}_{1-x}\text{Ga}_x\text{P}/\text{ZnS}$	475	20	49	4
	$\text{In}_{1-x}\text{Ga}_x\text{P}/\text{ZnS}$	465-475	42	56	5
Colloidal synthesis	$\text{In}_{1-x}\text{Ga}_x\text{P}/\text{ZnS}$	500	3	77	6
	$\text{In}_{1-x}\text{Ga}_x\text{P}/\text{ZnS}$	486	65	46	7
	$\text{In}_{1-x}\text{Ga}_x\text{P}/\text{ZnS}$	470	67	40	This work

Table S5 Summary on the EL properties of QLEDs fabricated with $\text{In}_{1-x}\text{Ga}_x\text{P}/\text{ZnS}$ QDs

EL peak wavelength (nm)	477
Turn-on voltage (V)	2.6
Maximum EQE (%)	0.56

Reference

- 1 K.-H. Kim, J.-H. Jo, D.-Y. Jo, C.-Y. Han, S.-Y. Yoon, Y. Kim, Y.-H. Kim, Y. H. Ko, S. W. Kim, C. Lee and H. Yang, Cation-Exchange-Derived InGaP Alloy Quantum Dots toward Blue Emissivity, *Chemistry of Materials*, 2020, **32**, 3537-3544.
- 2 X. Jiang, Z. Zhang, Z. Fan, D. Liu, S. Huang, L. Wang and B. Zou, A Double Zn and Ga Modification Strategy for Highly Efficient Deep Blue InP/ZnSeS/ZnS Quantum Dots, *ACS Applied Nano Materials*, 2024, **7**, 18714-18723.
- 3 V. Srivastava, V. Kamysbayev, L. Hong, E. Dunietz, R. F. Klie and D. V. Talapin, Colloidal chemistry in molten salts: Synthesis of luminescent $\text{In}_{1-x}\text{Ga}_x\text{P}$ and $\text{In}_{1-x}\text{Ga}_x\text{As}$ quantum dots, *Journal of the American Chemical Society*, 2018, **140**, 12144-12151.
- 4 K. D. Wegner, S. Pouget, W. L. Ling, M. Carrière and P. Reiss, Gallium—a versatile element for tuning the photoluminescence properties of InP quantum dots, *Chemical Communications*, 2019, **55**, 1663-1666.
- 5 D. Yoo and M.-J. Choi, Asymmetric Metal–Carboxylate Complexes for Synthesis of InGaP Alloyed Quantum Dots with Blue Emission, *ACS nano*, 2024.
- 6 J. Joo, Y. Choi, Y.-H. Suh, C.-L. Lee, J. Bae and J. Park, Synthesis and characterization of $\text{In}_{1-x}\text{Ga}_x\text{P}@\text{ZnS}$ alloy core-shell type colloidal quantum dots, *Journal of Industrial and Engineering Chemistry*, 2020, **88**, 106-110.
- 7 Y. Kim, K. Yang and S. Lee, Highly luminescent blue-emitting $\text{In}_{1-x}\text{Ga}_x\text{P}@\text{ZnS}$ quantum dots and their applications in QLEDs with inverted structure, *Journal of Materials Chemistry C*, 2020, **8**, 7679-7687.